University of Kentucky

UKnowledge

Physics and Astronomy Faculty Publications

Physics and Astronomy

8-30-2017

Inside-Out Growth or Inside-Out Quenching? Clues from Colour Gradients of Local Galaxies

Jianhui Lian
University of Kentucky

Renbin Yan
University of Kentucky, yanrenbin@uky.edu

Michael Blanton
New York University

Xu Kong
University of Science and Technology of China, China

Right click to open a feedback form in a new tab to let us know how this document benefits you.

Follow this and additional works at: https://uknowledge.uky.edu/physastron_facpub

Part of the Astrophysics and Astronomy Commons

Repository Citation

Inside-Out Growth or Inside-Out Quenching? Clues from Colour Gradients of Local Galaxies

Inside-out growth or inside-out quenching? Clues from colour gradients of local galaxies

Jianhui Lian,[1,2]★ Renbin Yan,[1] Michael Blanton[3] and Xu Kong[2]

[1]*Department of Physics and Astronomy, University of Kentucky, Lexington, KY 40506, USA*
[2]*CAS Key Laboratory for Research in Galaxies and Cosmology, Department of Astronomy, University of Science and Technology of China, Hefei, Anhui 230026, China*
[3]*Center for Cosmology and Particle Physics, Department of Physics, New York University, NY 10003, USA*

ABSTRACT

We constrain the spatial gradient of star formation history (SFH) within galaxies using the colour gradients in $NUV - u$ (where NUV stands for near-ultraviolet) and $u - i$ for a local spatially resolved galaxy sample. By splitting each galaxy into an inner and an outer part, we find that most galaxies show negative gradients in these two colours. We first rule out dust extinction gradient and metallicity gradient as the dominant source for the colour gradient. Then using stellar population models, we explore variations in SFH to explain the colour gradients. As shown by our earlier work, a two-phase SFH consisting of an early secular evolution (growth) phase and a subsequent rapid evolution (quenching) phase is necessary to explain the observed colour distributions among galaxies. We explore two different inside-out growth models and two different inside-out quenching models by varying parameters of the SFH between inner and outer regions of galaxies. Two of the models can explain the observed range of colour gradients in $NUV - u$ and $u - i$ colours. We further distinguish them using an additional constraint provided by the $u - i$ colour gradient distribution, under the assumption of constant galaxy formation rate and a common SFH followed by most galaxies. We find the best model is an inside-out growth model in which the inner region has a shorter e-folding time-scale in the growth phase than the outer region. More spatially resolved UV observations are needed to improve the significance of the result.

Key words: galaxies: evolution – galaxies: photometry – galaxies: star formation.

1 INTRODUCTION

The cosmic star formation history (SFH) of the universe is well established (Madau & Dickinson 2014). However, the SFH of individual galaxies that contribute to the cosmic SFH is not fully understood yet. For galaxies on the stellar mass-star formation rate (SFR, i.e. star formation main-sequence) relation, their SFH is relatively well determined and can be approximated by a single phase of exponential decline (Noeske et al. 2007). Generally, the SFR of star-forming galaxies declines slowly with cosmic time with an exponential time-scale typically longer than 10 Gyr (Noeske et al. 2007). Meanwhile, more massive galaxies tend to form at an earlier time and have SFR decreasing slightly faster. Off the main-sequence relation, the situation becomes complicated and unclear. Many previous works suggest that galaxies just leaving the star-forming main sequence

are experiencing a rapid decline of SFR (Faber et al. 2007; Martin et al. 2007; Balogh et al. 2011; Lian et al. 2016, hereafter Paper I) with a time-scale of the order of 1 Gyr (Schawinski et al. 2014) or even lower (Paper I). This rapid cessation process of SFR is distinctive from the secular evolution in the star-forming stage, and is often referred to as a 'quenching' process. This quenching process is necessary in galaxy evolution models to explain the galaxy distribution in NUV−optical (NUV stands for near-ultraviolet) colour–colour diagrams (Schawinski et al. 2014; Paper I) and the buildup of red sequence from $z = 1$ to 0 (Bell et al. 2004; Blanton 2006; Faber et al. 2007; Moustakas et al. 2013). In Paper I, we explored two key properties of the quenching process, the evolution speed during quenching and the quenching rate among star-forming galaxies, by analysing the galaxy distribution in $NUV - u$ versus $u - i$ colour diagram.

Aside from the unclear integrated SFH of galaxies, how the SFH of galaxies varies internally is still poorly understood. One direct probe of the internal variation of SFH is the spatial distribution of

★ E-mail: ljhhw@mail.ustc.edu.cn

colours, i.e. the colour gradient. Negative colour gradients have been found to be prevalent in nearby galaxies (e.g. Peletier et al. 1990). However, the physical origin of this colour gradient is not fully understood and is under debate. Spatial variations of galaxy properties other than the SFH are in principle able to produce the observed negative colour gradient, such as dust extinction (Liu et al. 2016) and stellar metallicity (Wu et al. 2005; Tortora et al. 2010). Therefore, it is important to understand the role played by these parameters and SFH in the colour gradient before we use this colour gradient to study the internal variation of SFH. After accounting for the contribution by dust extinction and stellar metallicity, the observed colour gradient could be used as a powerful tool to investigate the spatial variations of SFH in a galaxy. However, interpreting the colour gradient as a gradient in SFH is not straightforward since the SFH is usually complicated.

In addition, the phrase people use to describe the spatial variation in SFH within a galaxy is confusing the situation. Both 'inside-out growth' and 'inside-out quenching' can be found in the literature, most of the time without clear definitions. Some would even consider these two phrases as describing the same phenomenon. At the same time, the same phrase has been used to refer to different observation by different authors. For example, 'inside-out growth' has been used to refer to the growth of the disc truncation radius or scale radius (Azzollini, Trujillo & Beckman 2008), or the gradient in specific SFR (Wang et al. 2011).

In Paper I, we demonstrated that a two-phase SFH is necessary to explain the colour distribution of galaxies in $NUV − u$ versus $u − i$ diagram. One phase is a secular evolution phase with long time-scales, which we define as the 'growth' phase. It is followed by a second phase with a rapid decline of SFR on short time-scales, which we define as the 'quenching' phase. This allows us to clearly distinguish growth from quenching. In this work, we use the same SFH as in Paper I. To constrain the spatial variations in SFH, we use stellar population synthesis model with various spatial variations in SFH to reproduce the observed negative colour gradients. The models with spatial variation in SFH at the growth phase or the quenching phase are classified as 'inside-out growth' or 'inside-out quenching' models, respectively. As shown in Paper I, $NUV−$optical colours are sensitive to the quenching process and could be used to constrain the quenching properties. Thanks to the large sky area surveys of *Galaxy Evolution Explorer* (*GALEX*) in the UV band and SDSS in the optical band, the $NUV−$optical colour gradient is accessible for a statistically significant sample (Liu et al. 2016; Paper I). Throughout this paper, we adopt the cosmological parameters with $H_0 = 70 \,\mathrm{km\,s^{-1}\,Mpc^{-1}}$, $\Omega_\Lambda = 0.73$ and $\Omega_m = 0.27$. All magnitudes in this paper are given in the AB photometric system.

2 SAMPLE SELECTION

We select a local galaxy sample from NASA Sloan Atlas (NSA) catalogue (Blanton et al. 2011),[1] which provides SDSS and *GALEX* images, consistently measured photometry at the UV and optical bands, and rest-frame absolute magnitude at these bands after correcting for Galactic extinction and *k*-correction. It also provides axial ratio and position angle measurements determined from Stokes parameters at 90 per cent light radius. In this work, we consider the regions within 0.3 effective radius (r_e) of a galaxy as its inner part while the regions with $0.5r_e < r < r_e$ as the outer part. We
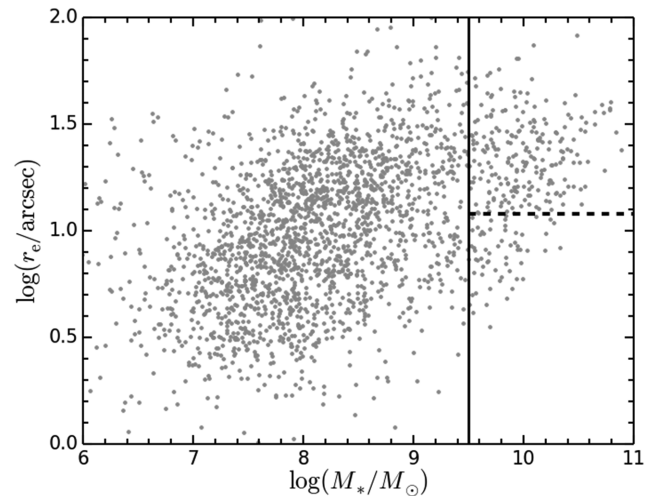
Figure 1. Mass-size relation of galaxies with redshift $z < 0.01$. The dashed horizontal line indicates the size limit required to resolve the inner part of galaxies, while the solid vertical line denotes the mass limit to ensure an acceptable mass completeness.

define these regions by elliptical shapes with identical axial ratios and position angles as those measured for the overall galaxy, which is given by the NSA catalogue. The gap between the two spatial parts is used to minimize the potential light contamination between them. We require the inner part ($r < 0.3r_e$) to cover at least one *GALEX* PSF (point spread function; full width at half-maximum of 5.3 arcsec at the NUV band) along its minor axis. Given the lower limit of the axial ratio we allow, this means a galaxy needs to have an effective radius $r_e > 12$ arcsec to be selected. With such a stringent requirement, we could only select nearby massive galaxies to ensure a reasonable mass completeness. Fig. 1 shows the distribution of galaxies with $z < 0.01$ in the mass–r_e diagram. The dashed horizontal line indicates the size limit required to resolve the inner part of galaxies. To achieve a relatively high completeness (i.e. high fraction of galaxies selected by the size criteria), a high lower limit on mass needs to be set due to the positive mass–size relation. To minimize intrinsic extinction, we focus on face-on galaxies with axial ratios b/a > 0.7. To summarize, the selection criteria for our galaxy sample are (1) stellar mass $M_* > 10^{9.5}\,\mathrm{M_\odot}$; (2) redshift $z < 0.01$; (3) effective radius $r_e > 12$ arcsec; and (4) axial ratio $b/a > 0.7$. Finally, 76 per cent of galaxies with mass above the threshold (229) objects are selected as our local spatially resolved galaxy sample. Among them, 102 galaxies with active star formation activity are detected in the *WISE W3* (12 µm) band.

3 DATA REDUCTION

For our galaxy sample, we use the *GALEX* and SDSS images provided by NSA (Blanton et al. 2011). *WISE* images, reduced and released by Lang (2014),[2] are also used to constrain the dust extinction in galaxies. To perform photometry in a consistent way, images in various wavelength bands need to be recentered to the same coordinate and converted into the same resolution level. We convolve the optical images with a Gaussian kernel to match the PSF of UV images and then rebin them to the same pixel size of 1.5 arcsec. To obtain the $W3 − NUV$ colour, we generate another
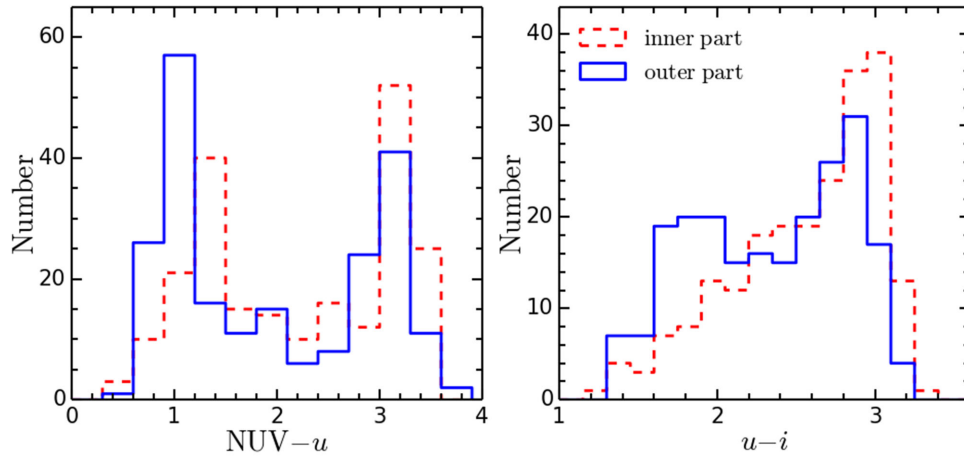
Figure 2. Number density profile of the inner and outer parts of galaxies in $NUV - u$ (left-hand panel) and $u - i$ colour (right-hand panel) space.

set of UV images that are converted into the same PSF (6 arcsec) and pixel size (2.5 arcsec) of *WISE* images.

For each galaxy in our sample, we measure the magnitudes of its inner and outer parts by summing the flux in the corresponding elliptical annulus. Since the *k*-correction is rather small for such nearby objects, with typical values less than 0.05 mag, we apply the correction factors derived from integrated magnitudes in the NSA catalogue to the inner and outer parts. The correction factor of foreground Galactic extinction is also taken from the NSA catalogue and assumed to be identical for the two parts of the same galaxy. As the measurements are obtained at fixed effective radius, we refer to the spatial variations of properties between the two parts as radial gradients.

4 COLOUR GRADIENTS AND THEIR PHYSICAL ORIGIN

4.1 Colour distribution

In Paper I, we discussed the $NUV - u$ colour distribution of galaxies in detail. In general, the distribution of galaxies in colour space is bimodal. Blue star-forming and red-sequence galaxy populations are separated by a wide low-density region called 'green valley'. The boundary of these three regions in colour space can be identified by significant number density drops, suggesting distinctive evolution stages of galaxies in these regions. Moreover, in order to reproduce the galaxy distribution in colour–colour space, we have to use a two-phase SFH with the second phase having much faster declining SFR. Fig. 2 shows the distribution of the inner and outer parts of galaxies in the $NUV - u$ and $u - i$ colour space, denoted by dashed red and solid blue lines, respectively. Interestingly, similar to the distribution of integrated colours in Paper I, the $NUV - u$ colour distribution of the two parts of galaxies are both bimodal. These common bimodal feature strongly suggests the inner and outer parts experience very similar two-phase SFH to the one adopted in Paper I. However, the inner parts are systematically redder than the outer parts in both $NUV - u$ and $u - i$ colour. In $NUV - u$, the median of the colour difference is 0.23 mag; in $u - i$, the median of the colour difference is 0.19 mag. This negative colour offset is consistent with previous work (Pan et al. 2014, 2016) where the authors found similar negative gradient in the NUV−optical colours in local

galaxies. Nevertheless, there is a small fraction of galaxies having blue star-forming outer part but red quiescent inner part.

4.2 Gradient in dust extinction

To investigate the origin of the negative colour gradient, we first explore the role played by the galaxy internal dust extinction. We obtain rough estimates of the dust extinction of the inner and outer parts using the IRX–A_{UV} relation (Meurer, Heckman & Calzetti 1999; Kong et al. 2004; Buat et al. 2005; Hao et al. 2011). The IRX index is defined as a flux ratio between the total infrared (TIR) and the UV [$L(TIR)/L(UV)$] bands. This index was proposed based on energy budget balance and has been widely used as a robust tracer of dust extinction. The $NUV-W3$ colour can be used as an approximation to the IRX index. The left-hand panel in Fig. 3 shows the distribution of $NUV-W3$ colour of the inner and outer parts, with median value of 4.37 ± 0.92 and 3.99 ± 0.82 mag, respectively. It can be seen that the inner parts are slightly redder than the outer parts in the $NUV-W3$ colour, indicating that they suffer more dust extinction.

To estimate the IRX index, we obtain the IR luminosity using the luminosity in the *WISE W3* band and the conversion from luminosity in a single mid-IR band to TIR luminosity proposed by Rieke et al. (2009). The IR luminosity calibration by Rieke et al. (2009) for the mid-infrared 12 μm band is based on the photometry in *IRAS* bands as $\log(L(TIR)) = (-0.947 \pm 0.324) + (1.197 \pm 0.034)\log(L(12))$. Because of the good agreement between the photometry in *WISE W3* and *IRAS* 12 μm band (Lian et al. 2014), we use the calibration in Rieke et al. (2009) directly to convert the luminosity into the *WISE W3* band to the total IR luminosity. Dividing the IR luminosity by the UV luminosity derived from the UV images, we obtain the IRX index for the two parts of galaxies. According to Buat et al. (2005), the dust extinction at the NUV band can be derived using the IRX index by the calibration $A_{NUV} = -0.0495x^3 + 0.4718x^2 + 0.8998x + 0.2269$, where x is the IRX index. Using this calibration, we acquire the extinction A_{NUV} as shown in the right-hand panel of Fig. 3 with median values of 4.30 ± 1.00 and 4.23 ± 0.86 for the inner and outer parts, respectively. The median offset is slight and not statistically significant, meaning a negligible negative gradient in dust extinction. Furthermore, assuming the extinction law of Cardelli, Clayton & Mathis (1989), we calculate the colour gradient introduced by this
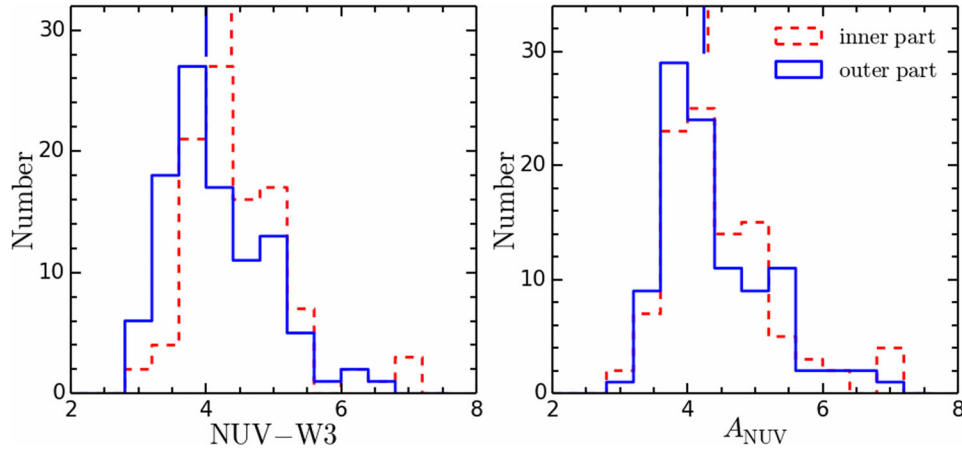
Figure 3. Left-hand panel: NUV−*W3* colour distribution of the inner and outer parts of galaxies. Right-hand panel: Extinction in the NUV band A_{NUV} distribution of the two parts. Vertical lines indicate the median value.
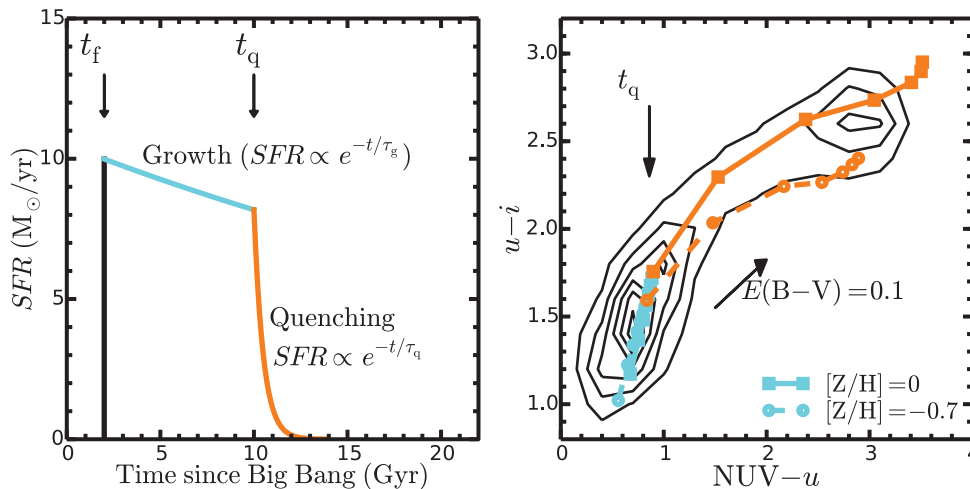

Figure 4. Schematic plot to show the two-phase SFH adopted in stellar population model. The left-hand panel shows the two-phase SFH definition and the four parameters that characterize the SFH. Cyan and orange lines denote the growth and quenching phase of the SFH, respectively. The right-hand panel shows this model's predictions for NUV − *u* versus *u* − *i* colours. The black contour represents the distribution of our galaxy sample. Squares represent the model with metallicity fixed to the solar value, while the circles are the model with sub-solar metallicity [Z/H] of −0.7 dex. The points on the model tracks denote the age of the model from 1 to 14 Gyr with an interval of 1 Gyr. The black arrow indicates the reddening caused by extinction with colour excess $E(B − V) = 0.1$.

slight gradient in extinction, which is 0.029 in $u − i$ and 0.043 in NUV − u, about 10 times lower than the observed colour gradients. Therefore, the dust extinction can be ruled out as the main driver of the observed colour gradient.

It should be noted that the dust extinctions derived above are just rough estimates and may not be precise enough to be used to correct the fluxes in the UV and optical bands. Comparing to the intrinsic dust extinction estimates based on stellar continuum fitting (Oh et al. 2011), our results overestimate the extinction by a factor of 2. There could be several possible reasons for this discrepancy. In deriving the total IR luminosity, we ignored the potential difference in *IRAS* 12 μm and *WISE W3* photometry. Another problem is that the total IR luminosity calibration may not be reliable in the low-IR luminosity region. This calibration is valid when $L(12\,\mu m) > 10^{8.5}\,L_{\odot}$ and will potentially overestimate the IR luminosity for objects with fainter $L(12\,\mu m)$. The majority of the inner and outer parts of galaxies in our sample have $L(12\,\mu m)$ within $10^{7.5}$–$10^{8.5}\,L_{\odot}$. Lastly, the IRX–A_{NUV} relation in Buat et al. (2005) is derived for a stellar population model with a chosen SFH that may not be representative to the galaxies in our sample. Although

these problems could affect the absolute value of dust extinction, the effect should be similar in the inner and outer parts of galaxies and the dust extinction gradient estimates should not be significantly biased.

4.3 Gradient in SFH

4.3.1 Stellar population model

In Paper I, we used a stellar population synthesis model and assumed an SFH with a two-phase exponential decline. The model can successfully reproduce the curved locus populated by galaxies in the colour–colour diagram and the NUV − *u* colour distribution. In this work, we use the stellar population model with a similar two-phase SFH to reproduce the colours of the inner and outer parts of galaxies. Here, we briefly introduce the parameters in the model. For more detailed description please see Section 4.1 in Paper I. There are four parameters in the two-phase SFH, galaxy formation time t_{f}, initial e-folding time at the growth phase τ_{g}, quenching start time t_{q}, and e-folding time τ_{q} at the quenching phase. The first two

parameters are for the growth phase and the last two are for the quenching phase. The left-hand panel of Fig. 4 shows a schematic plot of the two-phase SFH and illustrates the four free parameters. The growth phase and quenching phase of the SFH are denoted by cyan and orange lines, respectively. We generate model spectral energy distribution (SED) using Bruzual & Charlot (2003) model spectra with a Chabrier (2003) stellar initial mass function. Following the work by Schawinski et al. (2014), we exclude contribution by stellar population younger than 3 Myr because they tend to be surrounded by optically thick clouds and are not visible in the UV and optical. For the stellar metallicity in the model, we first adopt solar abundance ($Z = 0.02$).

As we found in Paper I, $NUV - u$ and $u - i$ colours can provide constraints on the parameters of the two-phase SFH. Generally, $u - i$ traces the average age of the stellar population while $NUV - u$ is more sensitive to the strength of the recent star formation activity. Combining these two colours could constrain how fast the SFR declines (i.e. the e-folding time) during the quenching phase. In the right-hand panel of Fig. 4, the black contour represents the distribution of galaxy sample in Paper I. It can be seen that the model reproduced the curved locus in the colour–colour diagram. For more discussion about the effects caused by different e-folding times at the growth and at the quenching phase, please refer to fig. 2 in Paper I.

It has been found that star-forming galaxies typically have a negative stellar metallicity gradient (González Delgado et al. 2015; Goddard et al. 2017a), which may contribute to the observed negative colour gradient (Wu et al. 2005; Tortora et al. 2010). To study the origin of the colour gradient, it is necessary to investigate the role played by the metallicity gradient. Therefore, we also generate another model with metallicity set to be -0.7 dex to investigate the potential colour gradient introduced by the negative metallicity gradient. In Fig. 4, the squares connected by solid line show the solar abundance model, while the circles connected by dashed line show the sub-solar abundance model. The colour scheme is the same as the left-hand panel to indicate the growth and quenching phase. It can be seen that the metal-poor model shows slightly bluer colour compared to the model with solar-abundance at the growth phase and much more significant colour difference at the quenching phase. During the growth phase, the maximum colour offset achieved at the growth phase by this 0.7 dex difference in stellar metallicity is $\sim$0.2 mag in $u - i$ and less than 0.1 mag in $NUV - u$. The variation in colour caused by the stellar metallicity gradient is much smaller than the observed colour gradients, especially in $NUV - u$. Moreover, the stellar metallicity gradient in star-forming galaxies is much flatter than -0.7 dex/r_e with a typical gradient of -0.1 dex/r_e (Goddard et al. 2017b). Although the colour difference caused by variation in stellar metallicity tends to be larger after the galaxy is quenched, the stellar metallicity gradient in passive galaxies is flatter than for star-forming galaxies (Goddard et al. 2017b). Therefore, we conclude that the stellar metallicity gradient cannot be the driver of the observed colour gradient.

4.3.2 Gradients in SFH

In previous sections, we found systematically negative colour gradients in our galaxy sample and excluded the gradient in dust extinction and stellar metallicity as the dominant drivers for the colour gradient. In this section, we further investigate what gradient in SFH could produce the observed colour gradients in most galaxies. Fig. 5 shows the $NUV - u$ and $u - i$ colour gradients as a function

of $NUV - u$ colour of the outer part in the first two columns and the relation between the two colour gradients in the third column. The data points represent individual galaxies and are identical in different rows of Fig. 5. According to the analysis in Paper I, the colour information of quiescent galaxies is not critical to constrain the SFH. In this figure, we exclude 89 galaxies with quiescent red outer parts (($NUV - u)_{outer} > 2.7$). This colour cut for quiescent galaxies is based on a clear number density drop at $NUV - u \sim 2.7$ found in Paper I.

It can be seen that most galaxies in our sample show a negative gradient in both $NUV - u$ and $u - i$ colour. This is consistent with the systematic shifts of colour distributions shown in Fig. 2. The colour gradient in $u - i$ seems to decrease as the outer part becomes redder in $NUV - u$, while no clear trend but large scatter can be found in the gradient in $NUV - u$. Interestingly, a minor fraction (30 per cent) of galaxies have positive colour gradients either in $NUV - u$ or $u - i$. These positive colour gradients may be due to gas infall in the centre that triggers star formation or stripping of the gas in the outer parts, suppressing the star formation. Investigating the origin of the positive colour gradient is not the goal of this work and we focus on the remaining 103 non-quiescent galaxies with negative colour gradient hereafter.

To investigate whether and how a gradient in SFH can reproduce the observed negative colour gradient, we generate four models of spatially varying SFH. In each model, we have two SFHs, one for the inner region and one for the outer region. As mentioned in Section 4.3.1, each SFH is described by four parameters. For simplicity, the two SFHs in each model share the same values for three of the four parameters and differ in only one of them. We refer to the varying parameter as the 'gradient' parameter. Each model explores a different 'gradient parameter' and is shown in each row of Fig. 5. The fourth column of Fig. 5 shows the SFHs adopted for the corresponding model. In contrast to the rest of the figure, in the first row we are varying the SFH of the outer part, while keeping the inner part fixed. The black line represents the SFH adopted for the outer part except for the model in the first row where the black line indicates the inner part. The other three coloured lines show three possible SFHs for the other part with the gradient parameter taking on different values. For clarity, a different normalization is adopted for each SFH. It should be noted that much more sophisticated models with more than one parameter varying might be less likely, but could to explain the colour gradient as well.

Initially, there are six free parameters in the each model, four parameters for one SFH, one additional parameter for the other SFH which has a different value, and dust extinction. For simplicity, the formation time of the inner part is fixed to be zero. The dust extinction is assumed to be $E(B - V) = 0.1$ to match the $NUV - u$ colour of galaxies in the horizontal direction. The number of free parameters is reduced to four. In this work, we do not intend to fit the data points one by one but explore the possible colour gradients that could be produced by the models. Therefore, we only show two or three models with a sparse grid in the 'gradient parameter'. When they are not used as a gradient parameter, t_f, t_q, τ_g, and τ_q are fixed to 0, 10, 40 and 0.8 Gyr, respectively.

Formation time t_f. In the first row of Fig. 5, we explore the colour gradient produced by different formation times t_f between the inner and outer regions, i.e. the gradient parameter in this model is the formation time. To produce the negative colour gradient, the inner part is required to form at an earlier time than the outer part. This is the first type of an 'inside-out growth' model named 'model A'. In this model, the gradient in $u - i$ colour reaches the maximum at the beginning when the outer part just forms and then
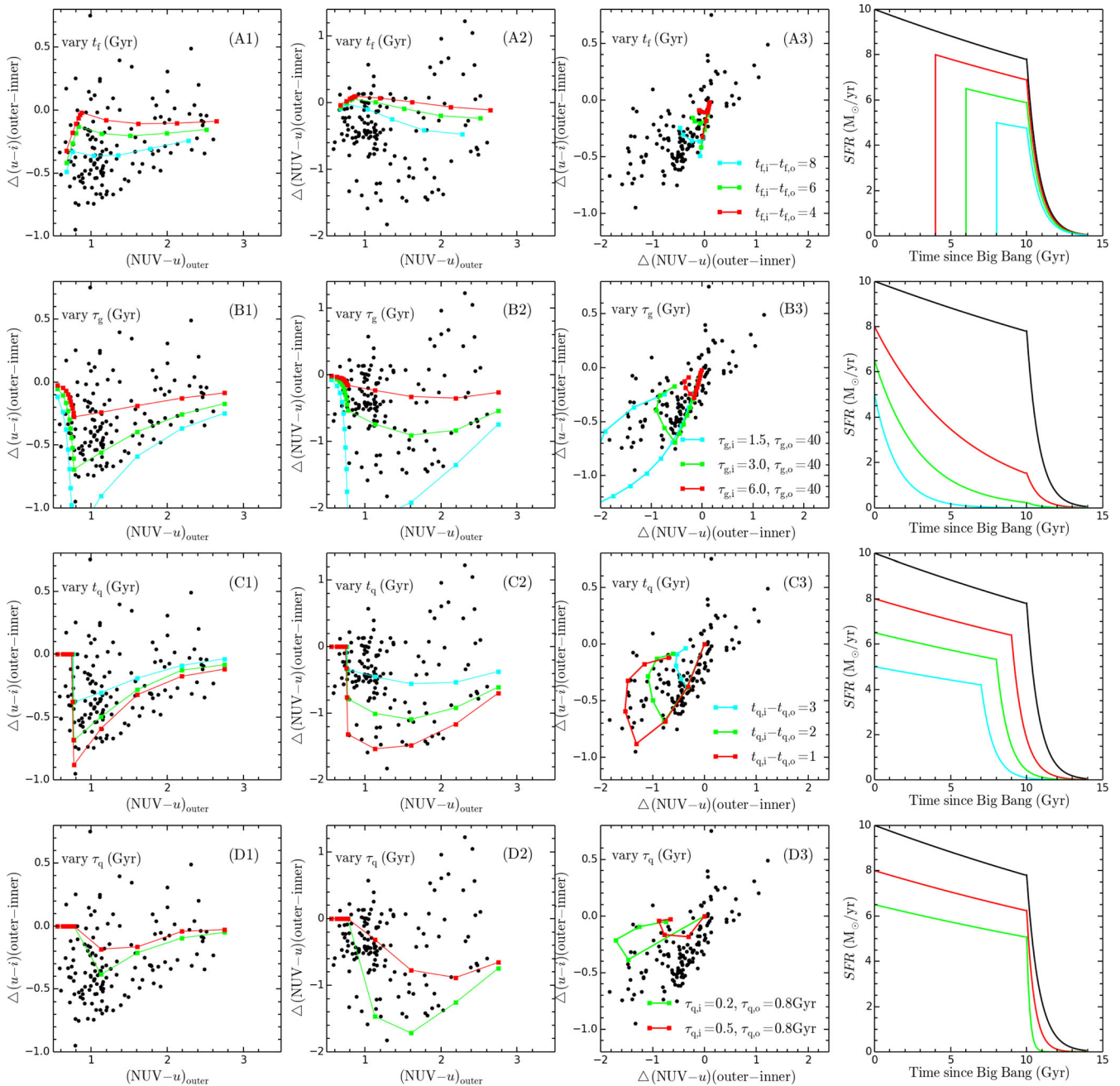
Figure 5. $u - i$ and NUV $- u$ colour gradients of local galaxies. Data points are identical in each row but overlaid with models of different 'gradient parameter'. The difference between the inner and outer parts in the gradient parameter is shown in the legend in the third column. First row: model A, outer parts form at later t_f. Second row: model B, inner parts have smaller τ_g with faster evolution speed during the growth stage. Third row: model C, inner parts start quenching at an earlier t_q. Bottom row: model D, inner parts have smaller τ_q with faster evolution speed during the quenching stage. The fourth column shows the SFH adopted for the corresponding model in each row. The black line represents the SFH adopted for the outer region except for the first row where the black line indicates the inner region. The coloured lines indicate the other region of the model galaxy with various choices for the gradient parameter.

monotonically decreases to zero when the outer part becomes quiescent with NUV $- u > 2.7$. The outer part is assumed to quench simultaneously with the inner part, suggesting a shorter growth phase due to a later formation. It can be seen that model A only produces slight or mild colour gradients, and fails to explain the galaxies with steep gradients, especially in NUV $- u$ colour. Changing the other free parameters does not improve the fitting significantly. Although model A cannot be totally ruled out as an explanation for the mild colour gradients observed in some galaxies, we conclude

that the observed colour gradients are not mainly driven by differing formation times between the inner and outer regions.

Growth e-folding time τ_g. In the second row of Fig. 5, we present the model with varying e-folding time at the growth phase τ_g, named 'model B'. In this model, the relatively redder colour of the inner part is due to its relative faster evolution during the growth phase. This is the second type of 'inside-out growth' model. The model colour gradient steepens during the growth stage and peaks when the quenching phase starts. The e-folding times of the outer part during
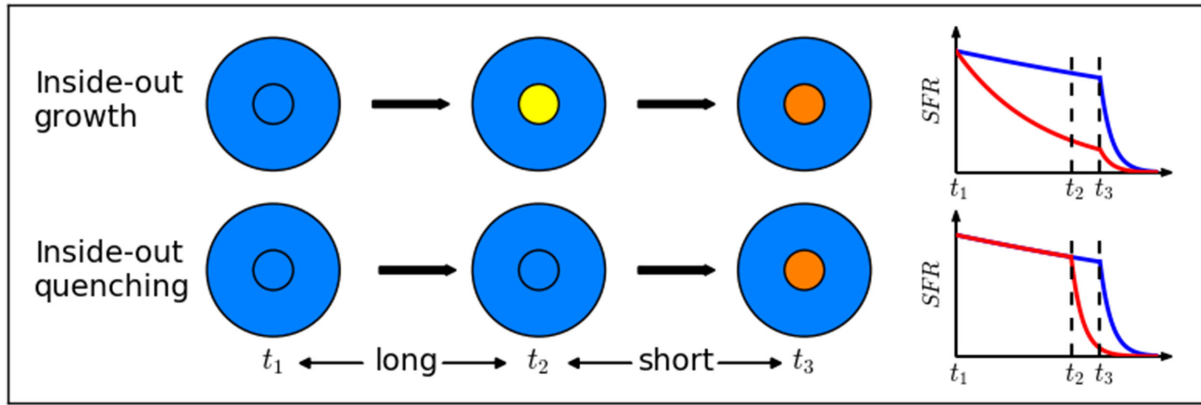
Figure 6. Schematic cartoon that shows the different colour gradient evolution history between the inside-out growth and inside-out quenching model. The inside-out growth model invokes different e-folding time at the growth phase τ_g between te inner and outer parts of galaxies, while the inside-out quenching model has a different quenching time t_q (See Fig. 5 and the text for more detailed discussion). The SFH of the two scenarios are also shown at the right-hand side. Blue and red lines represent the outer region and inner region, respectively.

the growth phase ($\tau_{g,o}$) is set to be 40 Gyr. This value is taken from Noeske et al. (2007), who derived the SFH for star-forming galaxies as a function of stellar mass by studying the cosmic evolution of mass-SFR (i.e. main-sequence) relation. As our galaxy sample has a median mass of $10^{9.92 \pm 0.28}\,\mathrm{M_\odot}$, we adopt the SFH of galaxies with stellar mass of $10^{10}\,\mathrm{M_\odot}$ in Noeske et al. (2007), which have an e-folding time of 40 Gyr. Model B can reproduce the observed negative colour gradients fairly well in both $NUV - u$ and $u - i$. Given our choices of other parameters, we find the inner part needs an e-folding time during the growth phase $\tau_{g,i}$ ranging in [3, 6] Gyr.

Quenching start time t_q. In the third row of Fig. 5, the 'gradient parameter' is the quenching start time t_q. In this scenario, to match the negative colour gradient, the inner part of galaxies needs to start quenching earlier than the outer part. This is our first type of 'inside-out quenching' model, named 'model C'. Before the inner part starts quenching, the colour gradients are zero because the SFH for the inner and outer parts are exactly identical. When the inner part starts quenching while the outer part is still in the growth stage, a dramatic negative gradient in $NUV - u$ colour and a mild negative gradient in $u - i$ colour develop within two or three Gyrs and peak at the moment when the outer region starts quenching. After that, the negative colour gradients begin to decrease until the outer part becomes quiescent. Like model B, model C also covers the observed negative colour gradients very well.

Quenching e-folding time τ_q. In the bottom row, we show the model with varying quenching e-folding time τ_q, called 'model D'. To produce negative colour gradient, the galaxy inner part needs to have a shorter e-folding time during the quenching phase. This is the second type of 'inside-out quenching' model. The quenching e-folding time of the outer part is set to be 0.8 Gyr. According to the findings in Paper I that, the typical quenching time-scales of local galaxies should be within the range of [0.2,1] Gyr. Changing the quenching time-scales within [0.2, 1] Gyr does not change our results significantly. Comparing to the observations, the colour gradient produced by model D is too steep in $NUV - u$ or too shallow in $u - i$ and deviates from the main distribution of galaxies as shown in panel D3 in Fig. 5. This mismatch cannot be improved by varying the other free parameters. Therefore, we conclude that the observed colour gradient cannot be driven by different e-folding time during the quenching phase between the inner and outer parts of galaxies.

To summarize, we find two models, one inside-out growth model (model B) with a gradient in the growth e-folding time and one

inside-out quenching model (model C) with a gradient in the quenching start time, are able to reproduce the ranges of observed negative colour gradients in $NUV - u$ and $u - i$. For convenience in the following discussion, we refer to our model B as the 'inside-out growth' model and model C as the 'inside-out quenching' model. The other two models with gradients in the other two parameters of the two-phase SFH fail to explain the observation and are ruled out. This result shows the power of colour gradients in $NUV - u$ and $u - i$ colour in differentiating variations of SFH across galaxies. However, the 'inside-out growth' and 'inside-out quenching' models cannot be distinguished only by the colour gradients. Other independent constraints are needed.

5 INSIDE-OUT GROWTH OR INSIDE-OUT QUENCHING?

Fig. 6 shows a schematic cartoon to illustrate the buildup history of the colour gradient and SFH for the inside-out growth and inside-out quenching models. The cartoon shows the colour of the inner and outer parts of two mock galaxies at three points in time. When the galaxy is just formed, no colour gradient exists, and both the inner and outer parts are blue. Later, the inner part of the mock galaxy with inside-out growth becomes redder than the outer part because the SFR of the inner part declines slightly faster. In contrast, the model galaxy with inside-out quenching still has zero colour gradient until the inner part start to quench. However, in the latter model, shortly after the inner part starts to quench at the time point t_2, it becomes much redder than the outer part rapidly.

As already shown in Fig. 5, the remaining 'inside-out growth' and 'inside-out quenching' models can explain the observed colour gradients by only varying the 'gradient parameter'. However, the gradients in these models show up at different evolutionary stages and last for different amounts of time. Thus, the two models should have significantly different predictions for the colour gradient distribution among galaxies. Previously, in Section 4 and Fig 5, we were only concerned with the range of the gradient values, rather than its exact distribution. Thus, the gradient distribution provides an additional, independent constraint. To differentiate the two models, we utilize the observed colour gradient distribution and compare it with the predictions of the models.

The left-hand panel of Fig. 7 shows the colour gradient in $u - i$ as a function of $NUV - u$ colour of the outer part. Only galaxies with
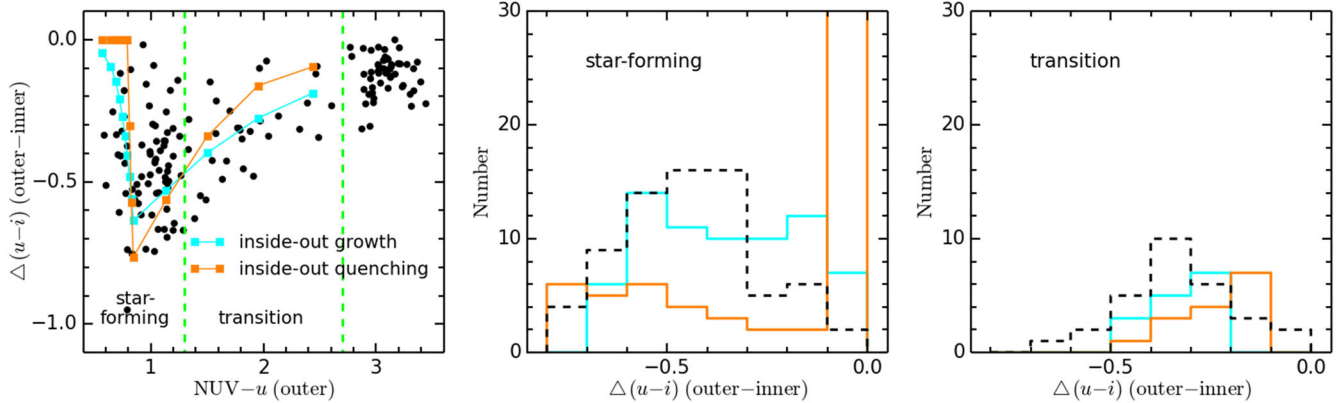
Figure 7. Left panel: colour gradient in $u - i$ as a function of $NUV - u$ colour of outer regions. Cyan and orange curves represent the adopted 'inside-out growth' and 'inside-out quenching' models, respectively. Green dashed lines indicate the boundary for separating galaxies during the star-forming or transition stages. Middle and right panel: $u - i$ colour gradient distribution for galaxies and models with $(NUV-u)_{outer} < 1.3$ (middle) and $1.3 < (NUV-u)_{outer} < 2.7$ (right-hand panel). Black dashed histograms represent the observed colour gradient distribution; cyan histograms are for the colour gradient distribution predicted by inside-out growth model; orange histograms are for the distribution of inside-out quenching model.

Table 1. Parameters adopted for the 'inside-out growth' and 'inside-out quenching' models in Fig. 7.

Model	$\tau_{g,i}$ (Gyr)	$\tau_{g,o}$ (Gyr)	$t_{q,o}$ (Gyr)	Δt_q (Gyr)	τ_q (Gyr)	$E(B - V)$
inside-out growth	3	10	10	–	1	0.1
inside-out quenching	–	10	10	3	1	0.1

negative colour gradient in both $NUV - u$ and $u - i$ are included in the plot. The green lines at $NUV - u = 1.3$ and $NUV - u = 2.7$ are used to divide the $NUV - u$ space into three regions, star-forming, transition and quiescent regions from the left to the right-hand side. The dividing boundary is adopted according to the number density drops in the $NUV - u$ colour distribution. The predictions of a typical 'inside-out growth' and 'inside-out quenching' models are shown in cyan and orange colour, respectively. The parameter adopted for the two models are listed in Table 1. As expected, the two models cover the observed colour gradient ranges equally well but develop the colour gradient differently. In the inside-out growth model, the negative colour gradient gradually increases during the growth stage, while in the inside-out quenching model the colour gradient increases dramatically after the inner part starts quenching and reaches its peak in a short time of 3 Gyr.

Due to this fast evolution of colour gradient, the inside-out quenching model cannot fit the colour gradient distribution of galaxies very well. On one hand, the inside-out quenching model suggests zero colour gradient for the first several Gyrs after galaxy formation. Assuming galaxies form with a constant rate at different epochs of the universe and follow the same SFH, in the inside-out quenching scenario, we should find many galaxies with zero colour gradients which, however, are not present in observation. It is hard to imagine, we are catching all galaxies during the brief moment of quenching (up to 3 Gyr at most) and they are all doing it simultaneously. On the other hand, judging from the age marks on the inside-out quenching model track, the model lasts for a similar time period with negative colour gradient at the star-forming and transition regions. With a constant galaxy formation rate, we should find similar numbers of galaxies in the two regions. However, by doing a simple counting, it is easy to find more galaxies with negative colour gradient located in the star-forming region compared to those in the transition region.

We demonstrate the above point quantitatively by comparing the observations and predictions of each model in the colour gradi-

ent distribution. Since the comparison is similar in the $u - i$ and $NUV - u$ colour gradient, for simplicity, we discuss only the comparison in the $u - i$ colour gradient. In each model, assuming a constant galaxy formation rate, we can compute how many galaxies we expect to observe with a certain colour gradient. When comparing to the data, we do the comparison for galaxies in star-forming region (defined by $NUV - u_{couter} < 1.3$) and transition region (defined by $1.3 < NUV - u < 2.7$) separately. The colour gradient distribution predicted by the models are derived by assuming a constant galaxy formation rate and counting the model points in each $u - i$ colour gradient bin. To be consistent with the data, the colour gradient distribution of models are also separated according to the same colour cuts, i.e. model points with $(NUV-u)_{outer} < 1.3$ are counted in the 'star-forming' panel and vice versa. Therefore, this comparison is not dependent on the choice of colour cut. The middle and right-hand panels of Fig. 7 shows the comparison in $u - i$ colour gradient distribution for the galaxies in star-forming and transition regions, respectively. The black dashed histograms represent the observed colour gradient distribution; cyan histograms are for the colour gradient distribution predicted by the inside-out growth model; orange histograms are for the distribution predicted by the inside-out quenching model. The distribution of the models can be scaled up and down by adopting different time grids. We adopt a time grid with 1 Gyr spacing for the models shown in the left-hand panel but a time grid with 0.15 Gyr spacing for the models in the middle and right-hand panels. The denser time grid (0.15 Gyr) is needed to roughly match the total number of observed galaxies.

The comparison confirms our previous interpretation that the 'inside-out quenching' scenario would yield an $u - i$ colour gradient distribution that does not match the observed distribution well. In contrast, the inside-out growth model predicts a flat colour gradient distribution in the star-forming region, which is consistent with the observation. Moreover, this model also reproduces more galaxies with negative colour gradient observed in star-forming than

transition region. Therefore, based on the $u - i$ colour gradient distribution, the inside-out growth scenario is preferred to the inside-out quenching scenario. For star-forming galaxies (middle panel of Fig. 7), the KS probabilities are 0.02 for the inside-out growth model and 1.35e-11 for the inside-out quenching model. For the transition galaxies, the KS probabilities are 0.74 for the inside-out growth model and 0.12 for the inside-out quenching model. This suggests that the inside-out quenching model is less favoured by the observations. The KS probability can only be considered in the relative comparison. And we should not take the absolute value too seriously as the model is overly simplistic. This analysis is limited by the sample size and more observations in spatially resolved UV imaging or spectroscopy are needed to increase the significance of the result.

The only way to resurrect the inside-out quenching model is to assume all galaxies formed at roughly the same time and they are all evolving synchronously. Based on the deep imaging and spectroscopic survey, the cosmic SFH is found to peak at $z \sim 2$ ($\sim$3.5 Gyr after big bang, Madau & Dickinson 2014) and decline significantly by an order of magnitude from the peak to now. However, the peak in the cosmic SFH at $z \sim 2$ should not be considered as an evidence for a peak formation of galaxies observed today. This is because the progenitor of today's star-forming galaxies may be too faint or even not yet formed to be counted in the cosmic SFH, which is obtained by deep surveys at $z \sim 2$ with typical mass completeness above $10^{9.5}$ M$_{\odot}$ (Madau & Dickinson 2014).

Regarding the assumption about a common SFH among all galaxies, although the inside-out growth scenario may be representative for most of the local star-forming galaxies, not all galaxies necessarily follow this SFH. As we mentioned in Section 4.1, many galaxies have blue star-forming outer parts but have red quiescent inner parts. These galaxies can also be identified in Fig. 5 with blue outer part (($\text{NUV}-u$)$_{\text{outer}}$ < 1.3) and distinctively steep $\text{NUV} - u$ colour gradient ($\triangle(\text{NUV} - u)_{\text{outer-inner}}$ < −1). In the second row with inside-out growth model B, the extremely steep $\text{NUV} - u$ colour gradient requires a very short e-folding time of 1.5 Gyr for the inner part, which is close to the e-folding time of 0.8 Gyr for the quenching phase. In these cases, the difference between the inside-out growth and inside-out quenching model becomes ambiguous. An inside-out growth model with extremely short e-folding time for the inner part could also be considered to be an inside-out quenching model. Since galaxies with such extreme colour gradient are rare and are only found in the left tail of the colour gradient distribution in Fig. 7, the comparison is not significantly affected by the potential deviation of SFH in these galaxies. Recently, Tacchella et al. (2015) studied a sample of massive star-forming galaxies at $z \sim 2.2$ with deep imaging and integral field unit observation. They found evidence for inside-out quenching in the most massive objects ($\sim 10^{11}$ M$_{\odot}$), which show similar surface mass density profiles to the local quiescent galaxies of the same mass range in the galaxy centre. Limited by the galaxy sample size, we are not able to further explore whether the preference of inside-out growth and inside-out quenching scenario is dependent on the stellar mass of galaxies. To significantly improve the spatially resolved sample, a high spatial resolution and wide-field UV imaging survey is needed.

6 SUMMARY

In this work, we investigate the internal variation of SFH across galaxies by analyzing the colour gradients in $\text{NUV} - u$ and $u - i$ for a local spatially resolved galaxy sample. We study the inner ($r < 0.3r_e$) and the outer ($0.5r_e < r < r_e$) regions in each galaxy.

The colour distribution of these two regions show a systematic offset. Generally, the outer parts of galaxies are bluer compared to the inner parts, confirming the negative colour gradient found in the local galaxies.

We first ruled out dust extinction gradient or metallicity gradients as the dominant cause of the colour gradients. To further explore the origin of the observed negative colour gradient, we use stellar population synthesis model and investigate the colour gradient predicted by radially varying SFHs in galaxies. We adopt a two-phase SFH that consists of a growth phase with long time-scale and a subsequent quenching phase with short time-scale. Compared to the observation, we find two simple scenarios can cover the observed negative colour gradient ranges in $\text{NUV} - u$ and $u - i$ equally well. In the first scenario, the inner regions of galaxies tend to evolve faster during the growth phase with a shorter time-scale compared to the outer regions and therefore the inside regions turn out to be redder. We call this model 'inside-out growth' model. In the other plausible scenario, the inner part of galaxies are redder because they cease their star formation (i.e. quench) earlier than the outer part. This model is called 'inside-out' quenching model.

To differentiate the inside-out growth and inside-out quenching scenario, we compare the observation with predictions of the two models in the $u - i$ colour gradient distribution. Since the colour gradients develop differently in the two scenarios, the colour gradient distribution predicted by the two models are therefore different. With assumptions of constant galaxy formation rate and a common SFH followed by most galaxies, the inside-out quenching model cannot reproduce the observed colour gradient distribution. In contrast, the colour gradient distribution predicted by the inside-out growth model is in good agreement with the observed distribution. Therefore, we conclude that the inside-out growth scenario is supported by the observed colour gradients of galaxies in $\text{NUV} - u$ and $u - i$. Nevertheless, we cannot rule out the possibility that a minor portion of galaxies, especially the massive ones (Tacchella et al. 2015), may experienced an inside-out quenching SFH. Moreover, the significance of the result is limited by the sample size and more spatially resolved UV observations are needed for a higher significance study. Besides, we urge all discussions on spatially resolved evolution studies to clearly define what is meant when speaking of 'inside-out growth' or 'inside-out quenching'.

REFERENCES

Azzollini R., Trujillo I., Beckman J. E., 2008, ApJ, 684, 1026
Balogh M. L. et al., 2011, MNRAS, 412, 2303
Bell E. F. et al., 2004, ApJ, 608, 752
Blanton M. R., 2006, ApJ, 648, 268
Blanton M. R., Kazin E., Muna D., Weaver B. A., Price-Whelan A., 2011, AJ, 142, 31
Bruzual G., Charlot S., 2003, MNRAS, 344, 1000
Buat V. et al., 2005, ApJ, 619, L51
Cardelli J. A., Clayton G. C., Mathis J. S., 1989, ApJ, 345, 245
Chabrier G., 2003, PASP, 115, 763
Faber S. M. et al., 2007, ApJ, 665, 265
Goddard D. et al., 2017, MNRAS, 466, 4731
Goddard D. et al., 2017, MNRAS, 465, 688
González Delgado R. M. et al., 2015, A&A, 581, A103
Hao C.-N., Kennicutt R. C., Johnson B. D., Calzetti D., Dale D. A., Moustakas J., 2011, ApJ, 741, 124
Kong X., Charlot S., Brinchmann J., Fall S. M., 2004, MNRAS, 349, 769
Lang D., 2014, AJ, 147, 108
Lian J., Zhu Q., Kong X., He J., 2014, A&A, 564, A84
Lian J., Yan R., Zhang K., Kong X., 2016, ApJ, 832, 29 (Paper I)
Liu F. S. et al., 2016, ApJ, 822, 25
Madau P., Dickinson M., 2014, ARA&A, 52, 415
Martin D. C. et al., 2007, ApJS, 173, 342
Meurer G. R., Heckman T. M., Calzetti D., 1999, ApJ, 521, 64
Moustakas J. et al., 2013, ApJ, 767, 50
Noeske K. G. J. et al., 2007, ApJ, 660, L47
Oh K., Sarzi M., Schawinski K., Yi S. K., 2011, ApJS, 195, 13
Pan Z., Li J., Lin W., Wang J., Kong X., 2014, ApJ, 792, L4
Pan Z., Zheng X., Lin W., Li Jinrong., Wang Jing., Fan Lulu., Kong Xu., 2016, ApJ, 819, 91
Peletier R. F., Davies R. L., Illingworth G. D., Davis L. E., Cawson M., 1990, AJ, 100, 1091
Rieke G. H., Alonso-Herrero A., Weiner B. J., Pérez-González P. G., Blaylock M., Donley J. L., Marcillac D., 2009, ApJ, 692, 556
Schawinski K. et al., 2014, MNRAS, 440, 889
Tacchella S., Carollo C. M., Renzini A. et al., 2015, Science, 348, 314
Tortora C., Napolitano N. R., Cardone V. F., Capaccioli M., Jetzer Ph., Molinaro R., 2010, MNRAS, 407, 144
Wang J., Kauffmann G., Overzier R. et al., 2011, MNRAS, 412, 1081
Wu H., Shao Z., Mo H. J., Xia X., Deng Z., 2005, ApJ, 622, 244

This paper has been typeset from a TEX/LATEX file prepared by the author.